Novel Wake-up Signaling for Enhanced Energy-Efficiency of 5G and beyond Mobile Devices

Soheil Rostami†*, Kari Heiska†, Oleksandr Puchko†, Jukka Talvitie*, Kari Leppanen†, and Mikko Valkama*

†Huawei Technologies Oy (Finland) Co. Ltd, Helsinki R&D Center
*Department of Electronics and Communications Engineering, Tampere University of Technology
Emails:†{soheil.rostami1, kari.heiska, oleksandr.puchko, kari.leppanen}@huawei.com,
*{soheil.rostami, jukka.talvitie, mikko.e.valkama}@tut.fi

***Abstract*—A low-power and low-latency communication system is vital to extend 5G mobile devices functionality, and to introduce innovative services and applications; on the contrary, limitations of state-of-the-art cellular subsystems prevent designing such a system based on current power saving mechanisms alone. In this paper, a new wake-up signaling for 5G control plane is introduced, aiming to reduce energy consumption of cellular subsystem in downlink. Performance of the proposed scheme in terms of false alarm and misdetection are investigated, and evaluated. The obtained numerical results show that such a signaling can reduce power consumption of discontinuous reception (DRX) by up to 30%, at the cost of negligible increments in signaling overhead.**

***Index Terms*—energy efficiency, mobile device, DRX, 5G.**

I. Introduction

Fifth generation mobile networks (5G) are expected to provide a diverse set of futuristic services such as augmented and virtual reality, cloud gaming and ultra-high-definition video streaming [1]. To satisfy the aggressive requirements of such services, advanced signal processing techniques and high bandwidth - ranges up to 400 MHz [2] - are imperative. Over the last decade, trend for increased bandwidth has been following the same exponential increase as Moore's Law for semiconductors. However, higher bandwidth communication consumes considerably higher power, and can exhaust the mobile devices battery power quicker. Due to fact that the battery evolution lags far behind changes in semiconductor industry with evidence of smartphones energy density has increased just a few percent during last decade [3], power saving methods are vital to extend 5G mobile devices functionality.

Multiple experimental investigations show that the most energy consuming components of smartphones can be attributed to the cellular subsystem and display [4], [5], [3]. Therefore, design of an energy-efficient cellular subsystem, conserving energy in battery is extremely paramount, and is main focus of our work.

This work has received funding from the European Union's Horizon 2020 research and innovation program under the Marie Skłodowska-Curie grant agreement No. 675891 (SCAVENGE), and Tekes TAKE-5 project.

Third generation partnership project (3GPP) specified DRX, as a promising solution for enhanced battery life by means of switching off RF circuitry and other modules for long periods, activating it only for short intervals. In spite of utilizing DRX in long-term evolution (LTE), it is not sufficiently energy efficient, and it still needs to be improved.

The main contribution of this paper is to introduce a novel narrow-band control plane signaling, referred to as wake-up signaling (WUS), in order to reduce energy consumption of mobile devices. In the proposed approach, a mobile device monitors WUS at the specific time instants and subcarriers, in order to decide whether to process upcoming physical downlink control channel (PDCCH) or not. Furthermore, a low-complexity wake-up receiver (WRx) is developed to decode the corresponding WUS, and to acquire its time and frequency synchronization.

This paper is organized as follows. Section II describes the reasons behind energy inefficiency of the DRX mechanism, and proposes wake-up scheme to further improve energy efficiency of cellular subsystem. WUS structure and its detection procedure are discussed in Sections III. These are followed by simulation results and conclusion in Sections IV and V, respectively.

II. Problem Description and Wake-up Scheme

Ideally, cellular subsystem is expected to transit from sleep to active state or vice versa sharply, as illustrated in dashed line in Fig. 1; however, because of hardware preparation time, cellular subsystem power consumption shape changes from purely ideal rectangular to a smooth contour without sharp edges as shown in solid line in Fig. 1. As a result, considerable amount of energy is wasted during start-up and power-down time during a DRX cycle, as depicted in gray area in Fig. 1. The slightly smoothed power consumption profile necessarily introduces an unavoidable lower sleep time than an ideal scenario, consequently reducing sleep ratio and increasing energy consumption of DRX.

Table I expresses the average transitional timings and power consumption states of both short and long DRX cycles based

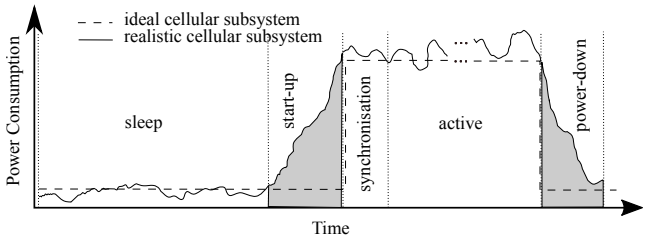

Fig. 1. Ideal and realistic power consumption of cellular subsystem in long DRX; in case of short DRX, start-up and power-down time is shorter, and required power for sleep period is higher, in addition, synchronization stage is not required, since the device is in-synchronization during sleep period of short DRX.

TABLE I
AVERAGE TRANSITIONAL TIME AND REQUIRED POWER CONSUMPTION OF LTE CELLULAR SUBSYSTEM DURING SHORT AND LONG DRX WHEN CARRIER BANDWIDTH IS 20 MHZ [6].

DRX Cycle	PW_{sleep}	t_{su}	PW_{active}	t_{sync}	t_{pd}
short	395 mw	1 ms	850 mw	0 ms	1 ms
long	9.8 mw	15 ms	850 mw	10 ms	10 ms

on average measurements of multiple different LTE cellular subsystems [6]. As it can seen, for short DRX cycle, sleep power consumption (PW_{sleep}) is much higher than long DRX cycle. This, in turn, has a direct influence on start-up time (t_{su}) and power-down time (t_{pd}). In case of short DRX, due to fact that baseband unit (BBU) is ON during sleep period, t_{su} and t_{pd} are shorter than long DRX. In short-DRX cycle, time required for synchronization t_{sync} is negligible. Required power for active state (PW_{active}), besides of implementation, varies based on bandwidth, and other communication parameters.

In respect to latency requirements, it is beneficial to process PDCCH in a very short DRX cycle to receive uplink (UL) grants or downlink (DL) data traffics, and promptly make an appropriate reaction. However, decoding the PDCCH requires a fast Fourier transform (FFT) whose size depends on the carrier bandwidth, and employs a blind decoding approach, where it hypothesizes over 44 options of PDCCH locations [7], [8]. Especially for higher bandwidth carriers, the PDCCH rendering is very computationally intensive and power consuming. Therefore, decoding PDCCH frequently, eradicates DRX advantages, and high power consumption overhead is inevitable.

It has been shown in [9] that the time period, that mobile device monitors channel without any data allocation has a major impact on battery consumption; for instance, according to the experimental results, video streaming and web browsing traffic as two key 5G use cases have empty PDCCH for 60% and 50% of time. Furthermore, this problem is severe in unloaded traffic scenarios, where many of DRX cycles have no data allocation for a particular mobile device. Therefore, reducing energy consumption of empty DRX cycles, has a significant potential to expand the battery life time of mobile devices.

In the proposed mechanism, the mobile device is configured with WRx in order to save battery life time, suitable for enhanced mobile broadband and massive machine type communication, which have small amounts of data at short intervals. In every wake-up cycle (w-cycle), WRx monitors physical downlink wake-up channel (PDWCH) for a specific on-duration time to determine if any data is scheduled or not. Occasionally, BBU based on the interrupt signal from WRx, switches on, decodes both PDCCH and physical downlink shared channel (PDSCH), and performs connected-mode procedures.

The WUS per each WRx is represented by 1-bit data, referred to as wake-up indication (WI), where 0 indicates WRx to not wake up BBU and 1 represents WRx to wake up BBU because there is a packet to receive. Each WI is uniquely code multiplexed before transmission to mobile devices. If 1 as WI has sent to WRx, network expects its corresponding mobile device to decode the PDCCH with time offset of t_{of}. In other words, PDWCH indirectly informs WRx of potential scheduling on PDCCH with time offset of t_{of} or rather if it can skip interrupting BBU for the rest of w-cycle. Fig. 2 depicts the operation and power consumption of the proposed cellular subsystem with WRx and conventional DRX-enabled cellular subsystem.

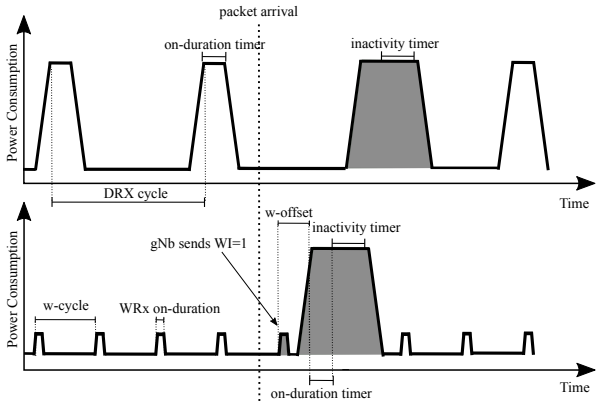

Fig. 2. Power consumption of typical DRX mechanism and WRx-enabled cellular subsystem.

BBU after receiving PDCCH message at active state for on-time duration, initiates its inactivity timer. After the inactivity timer is initiated, if a new PDCCH message is received before the expiration of inactivity timer, BBU re-initiates its inactivity timer. However, if there is no PDCCH message received before expiration of the inactivity timer, a sleep period starts, and the WRx-enabled cellular subsystem switches to its sleep state, and WRx operates according to its w-cycle.

The introduction of PDWCH has two unique consequences, misdetection and false alarm. In latter one, WRx wakes up in a predefined time instant, and wrongly identify 0 as 1 for WI, leading to unnecessary power consumption of BBU, thus the false alarm rate is required to be minimized. The former is corresponding to the case where 1 as WI is sent, but WRx decodes it as 0 incorrectly. The misdetection can

add an extra delay, and waste capacity in both PDCCH and PDSCH. Therefore, the probability of misdetection (P_{md}) requirement of PDWCH is stricter than probability of false alarm rate (P_{fa}). Simulation results in Section IV, verify that the proposed scheme can achieve P_{md} and P_{fa} almost zero for SNR larger than 0 dB.

III. Wake-up Signaling Structure and Detection

The proposed scheme is based on 5G access node (gNB) transmitting set of Zadoff-Chu (ZC) signatures with different cyclic shifts over a dedicated and pre-reported subcarriers, carrying set of WIs along with synchronization. A pool of known cyclic shift sequences is allocated to each gNB within a cell with a cell-specific root index, providing free inter-cell interference.

The ZC sequences have ideal cyclic auto-correlation, which is important for obtaining an accurate timing estimation and WRx identification. Additionally, the cross-correlation between different sequences based on cyclic shifts of the same ZC root sequence is zero at the WRx as long as the cyclic shift used when generating the sequences is larger than the maximum round-trip propagation time in the cell plus the maximum delay spread of the channel [10]. Root ZC sequence ($z^r[n]$) is a polyphase exponential ZC sequence with root index of r can be formulated as

$$z^r[n] = \exp\left\{-j\frac{\pi r n(n+1)}{K}\right\} \text{ for } n \in \{0, ..., K-1\}, \quad (1)$$

where K is odd-length of sequences, and needs to be integer larger than and relatively prime with respect to r [11]. An odd-length ZC sequence is symmetric to its center element, and enables design of hardware-efficient approach to generate. Further, if K is prime, the discrete Fourier transform (DFT) of $z^r[n]$ is another ZC sequence ($Z^r[k]$). For sake of readability, root index notation for the rest of this paper is omitted.

PDWCH is transmitted within the first symbol of subframe corresponds to the w-cycle. The main reason for transmitting PDWCH in the first symbol is to provide adequate time ($\leq t_{of}$) for WRx to possibly switch on BBU as early as possible. Therefore, BBU can prepare to decode PDCCH, and eventually, demodulate and decode PDSCH. This reduces the processing delay, and thus the overall DL transmission delay.

The multiple WIs are code multiplexed to a set of subcarriers; this structure enables efficient usage of radio elements, and reducing power consumption of WRx. We refer to a set of WIs transmitted on the same set of subcarriers as a PDWCH group.

We consider a multi-user single-cell scenario, where each sequence within PDWCH group is chosen from a set of M cyclic-shifted ZC sequences with length of K. Furthermore, during first OFDM symbol of predefined subframe, K contiguous subcarriers are utilized; the exact location of PDWCH is indicated by the frequency offset parameter. For simplicity's sake, we assume that subcarriers with relative indices to the DC subcarrier $k \in \{0, ..., K-1\}$ is used for PDWCH. Therefore, DFT of PDWCH group signal $Y[k]$ for M mobile devices is

$$Y[k] = Z[k] + \sum_{m=1}^{M} i[m]Z[k]\exp\left\{-j\frac{2\pi\tau[m]}{K}\right\}, \quad (2)$$

where $i[m]$ for $m \in \{1, ..., M\}$ is a binary variable, representing WI of m^{th} mobile device with its unique cyclic shift of $\tau[m] = mK_{cs}$, where $M \leq \lfloor K/K_{cs} \rfloor - 1$. $Z[k]$ is always transmitted within PDWCH group, helping WRx to retain synchronization regardless if $i[m] = 0, \ \forall m \in \{1, ..., M\}$. In Eq. (2) and in the rest of the paper, modulo-K indexing is assumed. The simplified PDWCH signal structure is illustrated in Fig. 3.

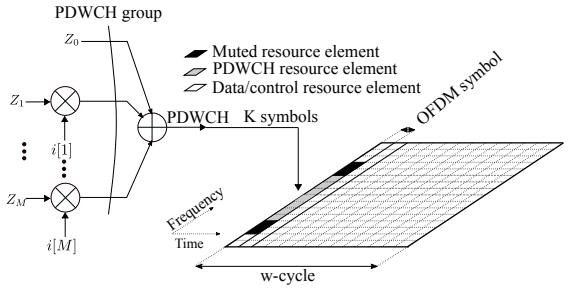

Fig. 3. Time-frequency grid illustrating PDWCH signal structure, Z_m refers to root ZC sequence with cyclic-shift of $\tau[m]$.

In the proposed scheme, high-power high-precise oscillator is kept ON, therefore implications of clock drift is negligible during short w-cycles. In order to further remove impact of any clock drift, the proposed receiver has two-stage mechanism to recover any potential symbol time offset (STO) and carrier frequency offset (CFO). At the first stage, which is performed in pre-FFT domain (time domain), maximum likelihood-estimator is applied to identify STO (δ) and fractional CFO (ϵ_f). After the synchronization of the symbol timing, cyclic prefix (CP) is removed correspondingly, and the second stage performed in FFT domain. In this work, we mainly focus on second stage, and first stage is not explained further (readers may refer to [13]).

Assuming that the initial synchronization provides an adequate orthogonality between subcarriers, N-point FFT output of q^{th} OFDM symbol is represented as $\mathbf{R}_q = [R_q[1], ..., R_q[K]]^T$. On the assumption that s is the index of OFDM symbol carrying PDWCH, $R_s[k]$ can be written as

$$R_s[k] = Y[k-\epsilon_i]H[k-\epsilon_i]\exp\left\{-j\frac{2\pi\upsilon(k-\epsilon_i)}{N}\right\} + W[k], \quad (3)$$

where υ denotes residual timing error - normalized by the sampling period - , $H[k]$ is the channel frequency response over the k^{th} subcarrier, and $W[k]$ is a circularly-symmetric white Gaussian process with average power σ_w^2. Without loss of generality for notational simplifications, we assume υ is incorporated into $H[k]$, therefore in the following, $\exp\left\{-j\frac{2\pi\upsilon}{N}\right\}$ from Eq. (3) is removed and absorbed as part of $H[k]$. Due to ambiguity of the arrival time of OFDM symbol

carrying PDWCH, WRx requires to observe x consecutive set of statistically independent FFT outputs $\mathcal{R} = [\mathbf{R}_1, ..., \mathbf{R}_x]$, in order to locate PDWCH symbol.

WRx at the second stage needs to perform three tasks, 1) to acquire the position of PDWCH symbol (s), 2) to receive its WI ($i[m]$), and 3) to obtain integer CFO (ϵ_i). In the following, we introduce an estimation method of unknown parameters $(\hat{s}, \hat{i}[m], \hat{\epsilon}_i)$.

In the proposed approach, WRx benefits from ideal cyclic auto- and cross-correlation properties of ZC sequences by computing received signal's power delay profile (PDP) through a frequency-domain matched filter. For this purpose, the squared of the correlation of the received q^{th} OFDM symbol with cyclic- and and phase-shifted of root ZC sequences is given by

$$\Psi_q(l, \epsilon_i) = \left| \sum_{n=0}^{K-1} r_q[n] z^*[n+l] \text{exp} \left\{ j \frac{2\pi \epsilon_i}{K} (n+l) \right\} \right|^2, \quad (4)$$

where $r_q[n]$ is equivalent time version of $R_q[k]$. As it can be seen from Eq. (4), the $\Psi_q(l, \epsilon_i)$ is maximum on the correct estimated CFO and PDWCH symbol. In order to reduce the implementation complexity, the hybrid time/frequency domain method is considered for the second stage. Using the properties of FFT, $\Psi_q(l, \epsilon_i)$ can be computed as

$$\Psi_q(l, \epsilon_i) = |\psi_q(l, \epsilon_i)|^2 = \left| \text{IFFT} \left\{ R_q[k] Z^*[k - \epsilon_i] \right\}_l \right|^2, \quad (5)$$

where $\psi_q(l, \epsilon_i)$ is the discrete periodic correlation function at lag l of received signal and complex conjugate of frequency-shifted of the root ZC sequence.

To make it clear, after removing CP at the first stage, and obtaining initial synchronization, $r_q[n]$ is translated to the frequency domain using N-point FFT, as shown in Fig. 4. Those K subcarriers corresponding to PDWCH are extracted from the output of the FFT using subcarrier demapper. The result of subcarrier demapping ($R_q[k]$) is multiplied by the complex-conjugate root ZC sequences with potential frequency offsets ($Z^*[k - \epsilon_i]$), and the result of each is oversampled - by factor of $L = 2^N/K$, where N is IFFT size - by padding zeros in order to balance between detection performance and implementation complexity. Next, the IFFT block, transforms the product of $R_q[k]$ and $Z^*[k - \epsilon_i]$ from frequency into time domain. And then, PDP samples are calculated by squaring of the absolute value of the time-domain data ($\psi_q(l, \epsilon_i)$). The received energy within the sliding window corresponding to m^{th} interval $m \in \{0, ..., M\}$, belonging to q^{th} OFDM symbol can be written as

$$E_q(m, \epsilon_i) = \sum_{l=mLK_{cs}}^{(m+1)LK_{cs}-1} \Psi_q(l, \epsilon_i). \quad (6)$$

Under the assumption that the LK_{cs} samples in the sliding window in the absence of WI are uncorrelated Gaussian noise with variance σ_w^2, therefore $\psi(l, \epsilon_i)$ also presents Gaussian distribution with zero mean and variance of $K\sigma_w^2$; consequently $\Psi(l, \epsilon_i)$ has a central Chi-squared distribution with 2 degrees of freedom with noise floor of $\beta = K\sigma_w^2$. Therefore,

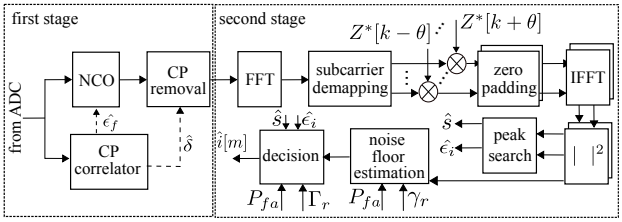

Fig. 4. Block diagram of main components of WRx.

the absolute WI detection threshold (Γ) can be calculated under the hypothesis of WI$= 0$ within a given P_{fa}, which can be written as

$$P_{fa} = 1 - F_1(\Gamma)^{LK_{cs}}, \quad (7)$$

where $F_1(\Gamma)$ is the cumulative distribution function (CDF) of Γ. Without loss of generality, we can assume that $\Gamma = \beta\Gamma_r$, where Γ_r is the threshold relative to the noise floor β; by doing such, dependency of $F_1(\Gamma_r)$ on the noise variance is removed, and can be modeled as a central Chi-squared random variable with $2LK_{cs}$ degrees of freedom [14]

$$F_1(\Gamma_r) = 1 - \text{exp}\{-\Gamma_r\} \sum_{k=0}^{LK_{cs}-1} \frac{1}{k!} {\Gamma_r}^k, \quad (8)$$

where Γ_r is a pre-computed coefficient, and stored in memory.

Similarly, the noise power samples at the input to noise floor estimation follows a central Chi-square distribution with 2 degrees of freedom

$$F_2(\Upsilon_r) = 1 - \text{exp}\{-\Upsilon_r\}, \quad (9)$$

where Υ_r is the relative detection threshold for noise floor estimation, and is set as follows

$$P_{fa} = 1 - F_2(\Upsilon_r), \quad (10)$$

and the absolute noise floor threshold (Υ) can be computed as

$$\Upsilon = \frac{F_2^{-1}(1 - P_{fa})}{N} \sum_{l=1}^{N} \Psi_q(l, \epsilon_i), \quad (11)$$

where F_2^{-1} is the inverse of CDF of F_2, and finally β is estimated as [15]

$$\beta = \frac{1}{N_s} \sum_{\substack{l=1 \\ \Psi_q(l,\epsilon_i) < \Upsilon}}^{N} \Psi_q(l, \epsilon_i), \quad (12)$$

where the accumulation is over all samples less than Υ, and N_s is the number of such samples.

Once the PDP samples of all potential frequency offsets of the root ZC sequence are obtained, $E_q(0, \epsilon_i)$ per frequency offset per OFDM symbol is calculated, and the corresponding frequency offset and index of OFDM symbol of the maximum of received energy is chosen as estimation of ϵ_i and s, respectively.

Then again by utilizing sliding window, if the received energy of estimated OFDM symbol in m^{th} interval ($E_{\hat{s}}(m, \hat{\epsilon}_i)$)

exceeds absolute WI detection threshold (Γ), m^{th} WRx declares realization of the $\hat{i}[m] = 1$, otherwise $\hat{i}[m] = 0$. Briefly, initially $(\hat{s}, \hat{\epsilon}_i)$ is obtained as follows

$$(\hat{s}, \hat{\epsilon}_i) = \underset{(s,\epsilon_i)\in\Theta}{\operatorname{argmax}}\{E_s(0, \epsilon_i))\} \tag{13}$$

and then

$$\hat{i}[m] = \begin{cases} 0, & \text{for } E_{\hat{s}}(m, \hat{\epsilon}_i) < \Gamma \\ 1, & \text{for } E_{\hat{s}}(m, \hat{\epsilon}_i) \geq \Gamma \end{cases} \tag{14}$$

on the assumption that (s, ϵ_i) is restricted to a given parameter space Θ. As it can be seen, accurate realization of the parameters in Eq. (13) requires a search over $x \times a$ values.

Because of very simple hardware architecture of WRx, in which is embedded in radio frequency integrated chip (RFIC) (rather than a discrete module), start-up and power-down time duration for WRx is extremely short, and it requires to just decode a few OFDM symbols and a few subcarriers in each w-cycle, in contrast to DRX, where BBU needs to operate full bandwidth for multiple symbols. In other words, narrowband reception of wake-up signaling requires less signal processing, consequently needs for less memories and operations. Moreover, its narrowband signal structure has higher sensitivity due to its low in-band receive noise.

In this work, power consumption of the realization of architecture for the WRx by integrating available LTE-optimized 16 nm CMOS-based RFIC is estimated. According to the pre-design estimation, it can consume up to 57 mW power, including its radio and digital processing, when $K = 117$ and $N = 128$, regardless of carrier bandwidth. Its required clock can be shared from the main BBU of cellular subsystem.

IV. Simulation Results

In this work, we consider 5G frame structure, where transmission over the subcarriers is arranged into frames of 10 ms long, each of which is divided into ten equally sized individual subframes, where each subframe is consisting of 14 consecutive OFDM symbols in the time domain, also in frequency domain, the subcarrier spacing equals 15 kHz. Additionally, within each frame, primary and secondary synchronization signals are utilized for network synchronization. Further, for simulation purposes, we adopt the extended pedestrian A model (EPA) developed by 3GPP [16], for the performance analysis and comparison. It is assumed that carrier bandwidth is 20 MHz, located in 900 MHz band.

Additionally, self-similar and long-range dependent traffic model, which is case for multimedia traffic, is utilized. For this purpose, the ETSI traffic model - widely is used in various analytical and simulation studies of 3GPP networks - is applied [17]. In the employed traffic model, a packet service session contains one or several packet calls with exponentially distributed session inter-arrival time with mean of 200 ms; each packet call itself consists of a sequence of packets with exponentially distributed packet call inter-arrival time, with mean of 10 ms. The mean session rate is one session per a minute.

Simulations are performed in an urban area, where the cell radius is 500 m, and mobile devices are distributed with uniform distribution within a single cell and single PDWCH group. Furthermore, each simulation scenario lasts for $100,000$ frames, and repeated $10,000$ times for averaging results. Each PDWCH group has $M = 7$ users (moving at a walking speed of 3 km/h), utilizing ZC sequences with length of $K = 117$ and root index of $r = 31$. We also assume $x = 3$, $a = 5$, and $K_{cs} = 13$. Finally, inactivity timer, on-time duration and offset time are considered as 12 ms, 1 ms, and 15 ms, respectively.

Fig. 5 shows a receiver operating characteristic (ROC) curve of the proposed wake-up scheme under EPA channel model at three different SNR values. As it can be expected, for all three ROC curves, there is a trade-off between P_{md} and P_{fa}. Furthermore, by comparing the ROC curves at different SNRs, we note that the P_{md} of SNR=-10 dB at $P_{fa} = 10\%$ is higher than that for SNR=-7 dB and SNR=-4 dB by 37% and 69%, respectively. As it can seen, for higher SNRs, ROC becomes closer to an ideal curve.

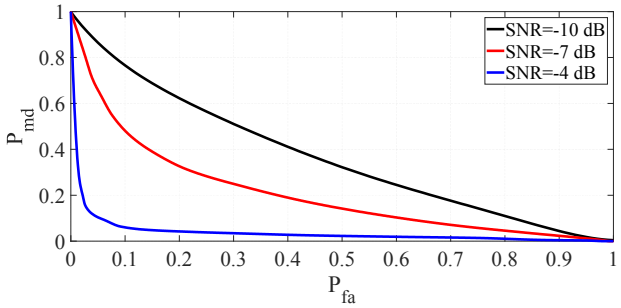

Fig. 5. ROC curves for three different SNRs.

The simulation results of P_{md} and P_{fa} for constant false alarm rates are indicated in Fig. 6. Similar to Fig. 5, for better SNR environments ($\geq$-2 dB), P_{md} reduces drastically. The misdetection rate for lower false alarm rate for a given SNR is higher than the corresponding misdetection rate of higher false alarm rate; implying the need for configuring the target false alarm based on the appropriate use cases energy and delay requirements.

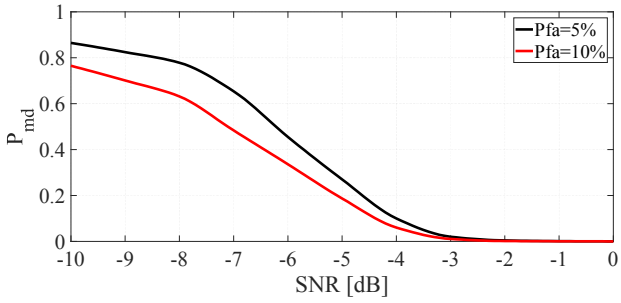

Fig. 6. Misdetection rate as a function of SNR, at fixed false alarm rates.

Moreover, Fig. 7 and Fig. 8 illustrate synchronization failure rate (P_{sf}) and mean squared error (MSE) of syn-

chronization failure as a function of SNR, respectively. As it can be expected, the failure rate reduces for higher SNR. Interestingly, the synchronization failure rate is not dependent on P_{fa}; and the main reason for such a trend is because of estimating ϵ_i without utilizing threshold (which is fixed based on target false alarm rate). Synchronization failure impacts directly on WI detection rate, and that is the main reason to reduce it as small as possible.

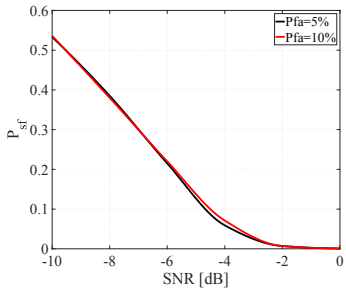

Fig. 7. Synchronization failure rate as function of SNR under different constant false alarm rates.

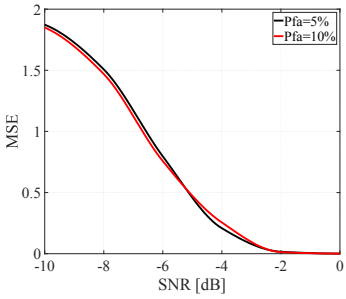

Fig. 8. MSE of ϵ_i normalized by subcarrier bandwidth as function of SNR under different constant false alarm rates.

Moreover, because of utilizing PDP values for selecting a PDWCH symbol, the probability of detection of the correct PDWCH OFDM symbol is almost 100%, even for low SNRs ranges -10 dB. The PDP of other OFDM symbols are extremely lower compared to the PDWCH symbol. It is very vital to have large PDWCH detection rate, since misdetection of PDWCH symbol can increase both false alarm and misdetection of WI directly.

Finally, the performance of WRx-enabled and DRX-enabled cellular subsystems, for different values of w-cycle and short/long DRX cycle length are compared. In addition, for fair comparison, we assume that DRX long cycle is four times of its short DRX cycle, and also short DRX timer is 16. Table. II shows the average delay and power consumption for aforementioned traffic model.

For low delay constraint, both methods consume higher energy, and main reason is that cellular subsystem remains in active state more than for case with longer delay constraint. As it can be seen from Table II, for same delay requirements, cellular subsystem with WRx demands much less power than DRX; for instance, if buffering delay constraint is 20 ms, by utilizing DRX, mobile device may achieve average power consumption of 158.8 mW, however with employing WRx, this can be reduced to 110.2 mW. However, power consumption of WRx approaches to DRX for very large or very short delays, and the reason is because of consuming higher energy for sleep state in WRx than deep sleep of long DRX cycle, and also due to overhead of start-up and power-down in very short w-cycles.

TABLE II
ACHIEVED VALUES OF POWER CONSUMPTION OF CELLULAR SUBSYSTEM WITH WRX AND DRX, ASSUMING THAT $P_{fa} = 0.1$ AND $P_{md} = 0.01$.

Delay	10 ms	20 ms	30 ms	40 ms	50 ms
WRx	211.6 mW	110.2 mW	94.86 mW	89.92 mW	87.72 mW
DRX	218.6 mW	158.8 mW	127.2 mW	109.6 mW	98.93 mW

V. CONCLUSION

In this paper, a novel wake-up scheme is proposed together with an efficient signal structure, such that reliable WUS detection, and thus large energy savings can be obtained in 5G and beyond mobile device. Link-level simulations are proposed in order to reduce the power consumption of DRX, by up to 30% for ETSI traffic model.

REFERENCES

[1] F. Boccardi, R. W. Heath, A. Lozano, T. L. Marzetta, and P. Popovski, "Five disruptive technology directions for 5G," *IEEE Communications Magazine*, vol. 52, no. 2, pp. 74–80, February 2014.

[2] S. Parkvall, E. Dahlman, A. Furuskar, and M. Frenne, "NR: The new 5G radio access technology," *IEEE Communications Standards Magazine*, vol. 1, no. 4, pp. 24–30, Dec 2017.

[3] M. Lauridsen, P. Mogensen, and T. B. Sorensen, "Estimation of a 10 Gb/s 5G receiver's performance and power evolution towards 2030," in *Proc. IEEE VTC 2005 Fall*, Sept 2015, pp. 1–5.

[4] "Designing mobile devices for low power and thermal efficiency," Qualcomm Technologies, Inc., Tech. Rep., Oct. 2013.

[5] A. Carroll and G. Heiser, "An analysis of power consumption in a smartphone," in *Proc. USENIXATC2010*. Berkeley, CA, USA: USENIX Association, 2010, pp. 21–21.

[6] M. Lauridsen, L. Noel, T. Sorensen, and P. Mogensen, "An empirical LTE smartphone power model with a view to energy efficiency evolution," *Intel Technology Journal*, vol. 18, no. 1, pp. 172–193, 3 2014.

[7] "Evolved universal terrestrial radio access (E-UTRA); physical layer procedures," 3GPP, TS 36.213, Tech. Rep., Mar. 2014.

[8] "Evolved universal terrestrial radio access (E-UTRA); user equipment (UE) procedures in idle mode," 3GPP, TS 36.304, Tech. Rep., Jan. 2016.

[9] "UE power consideration based on days-of-use," Qualcomm Incorporated, R1-166368, Tech. Rep., Aug. 2016.

[10] S. P. Erik Dahlman and J. Skold, *4G LTE/LTE-Advanced for Mobile Broadband*. Academic Press, 2011.

[11] J. C. Guey, "The design and detection of signature sequences in time-frequency selective channel," in *Proc. IEEE PIMRC 2008*, Sept 2008, pp. 1–5.

[12] M. H. Nassralla, M. M. Mansour, and L. M. A. Jalloul, "A low-complexity detection algorithm for the primary synchronization signal in LTE," *IEEE Transactions on Vehicular Technology*, vol. 65, no. 10, pp. 8751–8757, Oct 2016.

[13] J. J. van de Beek, M. Sandell, and P. O. Borjesson, "ML estimation of time and frequency offset in OFDM systems," *IEEE Transactions on Signal Processing*, vol. 45, no. 7, pp. 1800–1805, Jul 1997.

[14] J. G. Proakis and D. K. Manolakis, *Digital Signal Processing (4th Edition)*, 4th ed. Prentice Hall, Apr. 2006.

[15] S. Sesia, I. Toufik, and M. Baker, *LTE, The UMTS Long Term Evolution: From Theory to Practice*. Wiley Publishing, 2009.

[16] "LTE; evolved universal terrestrial radio access (E-UTRA); relay radio transmission and reception," 3GPP TS 36.16 version 11.4.0 Release 11, Tech. Rep., Apr. 2015.

[17] "Universal mobile telecommunications system (UMTS); selection procedures for the choice of radio transmission technologies of the UMTS," UMTS 30.03 TR 101 112, V3.1.0, Tech. Rep., Apr. 1998.